INFECTION AND IMMUNITY, May 1979, p. 508-522
0019-9567/79/05/0508-15$02.00/0

Vol. 24, No. 2

New Strain of Mouse Hepatitis Virus as the Cause of Lethal Enteritis in Infant Mice

JOHN C. HIERHOLZER,* J. ROGER BRODERSON, AND FREDERICK A. MURPHY†

Bureau of Laboratories, Center for Disease Control, Atlanta, Georgia 30333

Received for publication 2 February 1979

A new strain of mouse hepatitis virus (MHV) was isolated from pooled gut suspensions from an epizootic of lethal enteritis in newborn mice. Negative-contrast electron microscopy showed an abundance of coronavirus particles in the intestinal contents and intestinal epithelium of moribund mice. We found no other virus in the epizootic. Dams seroconverted to MHV polyvalent antigen and to the agent isolated, but did not develop antibodies to other known mouse pathogens. Virus propagated in NCTC-1469 tissue culture produced enteric disease in suckling mice but not fatal diarrhea; the dams of these mice also developed antibodies to MHV and to the isolates. By complement fixation, single radial hemolysis, and quantal neutralization tests, we found the isolates antigenically most closely related to MHV-S, unilaterally related to MHV-JHM, and more distantly related to MHV-1, MHV-3, MHV-A59, and human coronavirus OC-43. We also studied cross-reactions among the murine and human coronaviruses in detail. Tissues of infected newborn mice were examined by light microscopy, thin-section electron microscopy, and frozen-section indirect immunofluorescence, revealing that viral antigen, virus particles, and pathological changes were limited to the intestinal tract. We have designated our isolates as MHV-S/CDC.

Epizootics of newborn diarrhea have been a problem in mouse breeding colonies for many decades (2, 13, 33, 42, 50, 51). Until recently, epizootics which could not be associated with protozoa or bacteria were presumed to be of viral etiology, although specific etiological diagnosis was often not understood. In recent years, however, the role of specific viral agents has been clarified. Reovirus is a major cause of murine diarrhea (9). A second agent, epizootic diarrhea of infant mice (EDIM) virus, is the cause of diarrheal disease with a different infection pattern (33). A third virus, lethal intestinal virus of infant mice (LIVIM), first described by Kraft in 1962, is probably the most important viral agent of diarrheal disease in newborn mice (32). Kraft found that the virus is <300 nm in diameter by filtration; is sensitive to heat, ether, deoxycholate, and storage at 4°C; does not replicate in conventional cell cultures; and does not agglutinate avian and mammalian erythrocytes (RBC) (32). The agent is serologically distinct from EDIM virus, now known to be a rotavirus (26), and from reovirus; Kraft maintained that the intestinal pathology caused by this virus is pathognomonic (6, 32, 33).

† Present address: College of Veterinary Medicine and Biomedical Sciences, Colorado State University, Ft. Collins, CO 80523.

Investigators have not identified the virus or viruses responsible for LIVIM disease, although they have suggested an involvement with mouse hepatitis virus (MHV). In 1963, Rowe et al. described a contagious infection of newborn mice caused by an enterotrophic "S" strain of MHV; they found a degeneration of the tips of intestinal villi which resembled that found in LIVIM disease (50). They later thought that LIVIM disease might be an interaction between the EDIM agent and MHV (J. C. Parker and W. P. Rowe, personal communications, 1967). Outbreaks of LIVIM diarrheas in the mouse colony at the Center for Disease Control (CDC) in June 1965, January 1966, and June 1966 showed serological evidence of MHV infection (C. H. Calisher, unpublished data, 1967). During a recent epizootic of newborn diarrhea, shown histopathologically to be LIVIM disease, in this same colony we found large numbers of coronavirus particles in the intestinal contents of moribund animals (8). In this report we describe virological and pathogenetic characteristics of this epizootic and show its association with an antigenically distinct strain of MHV.

MATERIALS AND METHODS

Mice. Outbred ICR (CDC) mice were bred in a pathogen-free closed colony at the Lawrenceville, Ga.,

facility. The colony was continuously monitored and was negative for viral and bacterial pathogens at the time of the epizootic.

Pathology. Tissues of suckling and adult mice were embedded and stained with hematoxylin-eosin by standard procedures. Selected tissues were embedded for thin-section electron microscopy and examined at 60 kV in a Philips EM-300 microscope (41).

Negative-contrast electron microscopy. Fresh intestinal contents of suckling mice and tissue culture harvests of the virus isolates were stained by the droplet method with 2% potassium phosphotungstate at pH 7.0.

Tissue culture. NCTC-1469 cells, obtained from Microbiological Associates, Bethesda, Md., were grown under NCTC-109 medium with 20% horse serum and additives and maintained at 35°C under NCTC-109 medium with 10% horse serum and additives (all obtained from Microbiological Associates). After inoculation this medium was replaced with an "MHV maintenance" medium: Eagles minimal essential medium with 2% fetal calf serum, 2 mM L-glutamine, 1 mM sodium pyruvate, 0.065% bicarbonate, 100 U of penicillin per ml, 0.05 mg of streptomycin per ml, 0.002 mg of amphotericin B per ml, and 1× nonessential amino acids (0.1 mM each of alanine, asparagine, glutamic acid, glycine, proline, and serine).

Property tests. Acid, chloroform, and heat stability tests, deoxyribonucleic acid inhibitor tests, and other property tests used in virus classification were carried out in NCTC-1469 cells as described elsewhere (20, 21).

Viruses and antisera. Cultures of MHV strains and strain-specific mouse antisera were kindly furnished by Michael Collins and John Parker of Microbiological Associates. Polyvalent MHV antigen and antiserum and reagents for other common murine pathogens came from Microbiological Associates or from our own stocks. MHV-S/CDC antisera were six separate pools of serum from dams who had cannibalized their infected offspring 3 weeks earlier. Antisera to human coronavirus OC-43 and 229E have been described previously (20, 23, 25).

Serological tests. Complement-fixation (CF) tests were performed with overnight fixation of 5 U of complement (11). Hemagglutination and hemagglutination inhibition (HI) assays were performed with 0.4% mammalian and 0.5% avian RBC and 0.01 M phosphate-buffered saline diluent (24). Infectivity titrations and serum neutralization tests were done in replicas of five in NCTC-1469 cells and read by cytopathology after 5 days of incubation of 35°C. Immunodiffusion tests were performed as described for other coronaviruses (20, 23), counterelectrophoresis was performed as described for adenoviruses (22), and single radial hemolysis was performed as described for nonhemagglutinating viruses (25). We performed indirect fluorescent antibody tests on whole-mouse frozen sections as described elsewhere (4). Briefly, we fixed air-dried sections with acetone (10 min, 23°C) and covered with mouse antisera to the MHV-S/CDC isolates, to the prototype MHV strains, or to the polyvalent antigens (30 min, 23°C). We washed the sections and incubated them for 30 min with goat anti-mouse immunoglobulin G globulin (Meloy, Springfield, Va.). For all serological tests we inactivated the antisera at 56°C for 30 min.

RESULTS

Epizootic. In March 1976 a devastating epizootic of diarrheal disease occurred in the CDC mouse colony. The disease occurred when mice purchased from many outside sources inadvertently came in contact with a nursery used to produce suckling mouse litters for viral studies. High mortality during the first 7 to 10 days of life characterized the epizootic, which did not clinically affect the mothers or the purchased mice. Mothers cannibalized their litters within a few hours after death. Stringent use of filter tops on cages, disinfection, and physical and air barrier separation of separate mouse groups controlled the epizootic.

To find the etiology of this outbreak, we expressed the intestinal contents from moribund mice and examined them by negative-contrast electron microscopy. We observed large numbers of coronavirus particles (Fig. 1). The particles were 100 to 130 nm in diameter and had the large petal-shaped surface projections characteristic of coronaviruses. Despite extensive searching, we found no evidence of EDIM virus or any other virus.

The disease was easily passed by touching the noses of newborn mice to feces of affected mice. We made serial passages for virus production and tissue studies. Third- through seventh-passage mice were thus obtained and frozen at −70°C when they became moribund with severe diarrhea 4 or 5 days after exposure to the virus.

Pathology. Moribund suckling mice lacked normal pink skin color, became dehydrated, and were often soiled with feces. At necropsy, the intestines were flaccid and contained variable amounts of watery, yellowish material. Only the intestines showed histological changes. The villi of the lower small intestine were markedly blunted due to destruction of surface (absorptive) epithelium. Many multinucleated giant cells, such as Kraft described (32), were seen in association with the degeneration of villous epithelium (Fig. 2). Eosinophilic intracytoplasmic inclusion bodies were seen in affected epithelium and syncytial cells (Fig. 3). In some cases lesions were observed in the colon, with epithelial cell degeneration, multinucleate cell formation, and diffuse mucosal inflammatory cell infiltration (Fig. 4). Cuboidal metaplasia was often associated with these lesions.

Thin-section electron microscopy revealed large numbers of coronavirus particles in intestinal epithelium and in macrophages of the lamina propria of the jejunem and ileum. The virus

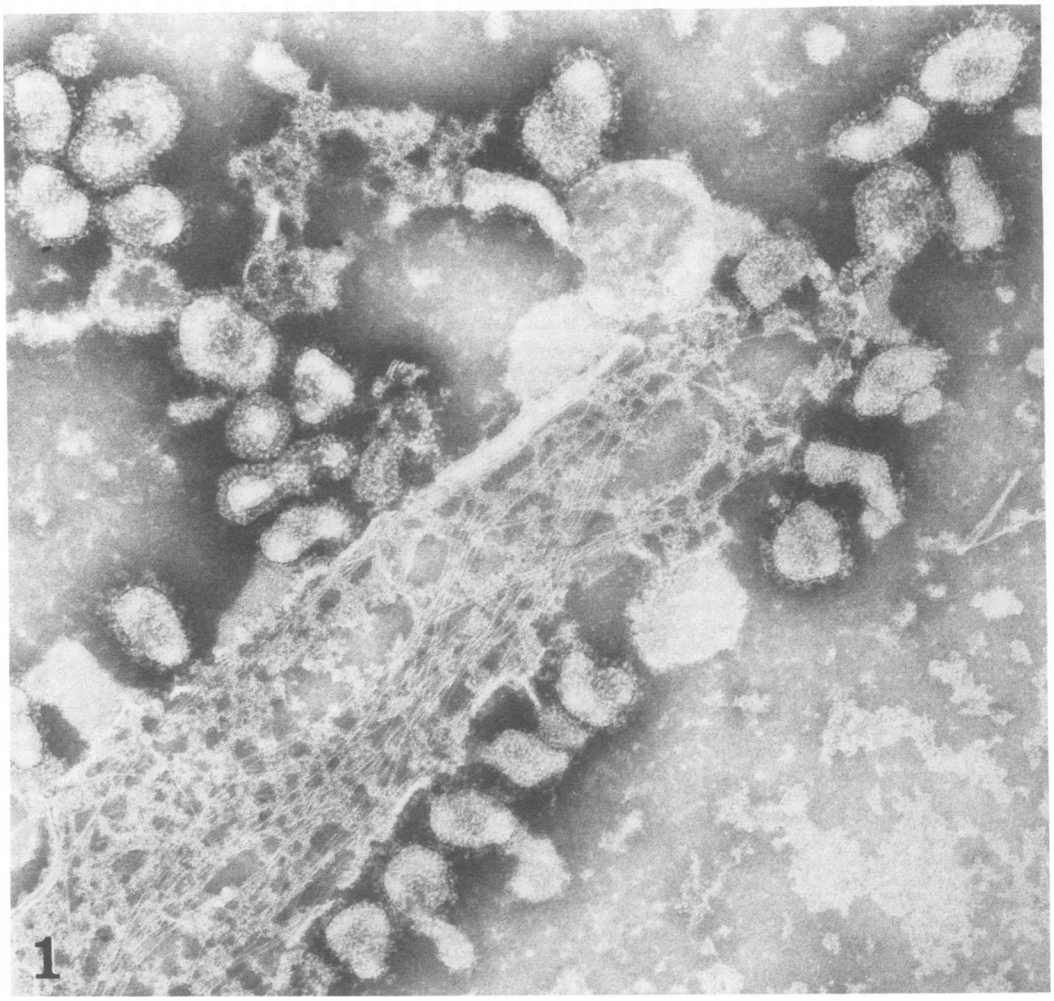

FIG. 1. *Negative-contrast electron microscopy of intestinal contents showing numerous coronavirus particles, many of which are lined up along a meshwork of fibrin strands. ×86,400.*

particles (Fig. 5) were associated with cell degeneration and necrosis (Fig. 6). The inclusion bodies seen by light microscopy were observed by electron microscopy as amorphous bodies in degenerating epithelium and syncytial cells (Fig. 7).

Frozen-section immunofluorescence showed viral antigen in these inclusions; in most cases, antigen also filled the cytoplasm of infected epithelial cells (Fig. 8). The pattern of immunofluorescence was constant even though many antisera were used on whole-mouse sections. In each case only gut tissue stained, and it stained equally well with MHV polyvalent antiserum, with MHV-S/CDC antisera, and with antisera to the five MHV strains.

In the dams of affected litters, only the liver exhibited pathological changes. Small foci of necrosis with mixed inflammatory infiltrations appeared as early as 5 days after exposure.

Preliminary serology. We held mice which had cannibalized their litters for 3 weeks and then tested their sera for antibodies to common murine pathogens. The CF test indicated titers as high as 1:128 with MHV polyvalent antigen, but neither CF nor HI tests showed any significant titers with other antigens (see Tables 1 and 2). Preepizootic sera of mice randomly selected from the colony for routine testing exhibited no CF or HI antibody titers to any of the agents listed. In reciprocal tests, antigens prepared from gut suspensions of moribund suckling mice gave the same titers with MHV polyvalent antiserum as did positive control MHV antigens. Gut suspensions from normal control mice did not react beyond a low anticomplementary level with

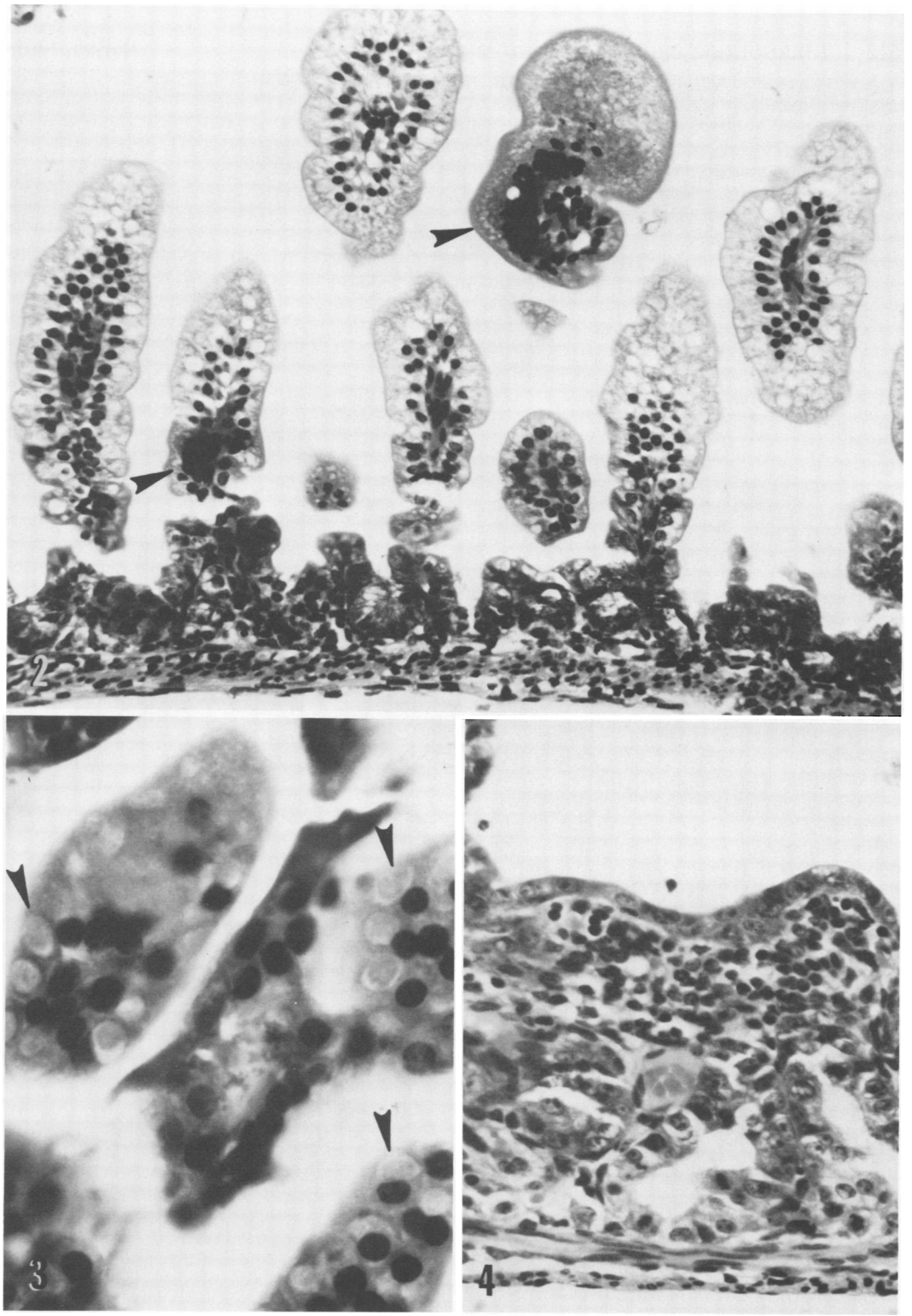

FIG. 2. *Section of small intestine showing degeneration of villi with formation of syncytial cells (arrows). ×276.*

FIG. 3. *Degenerating villus epithelium showing many cytoplasmic inclusions (arrows). ×672.*

FIG. 4. *Mucosa of the colon is infiltrated with many leukocytes. Surface is partially covered with cuboidal epithelium. ×328.*

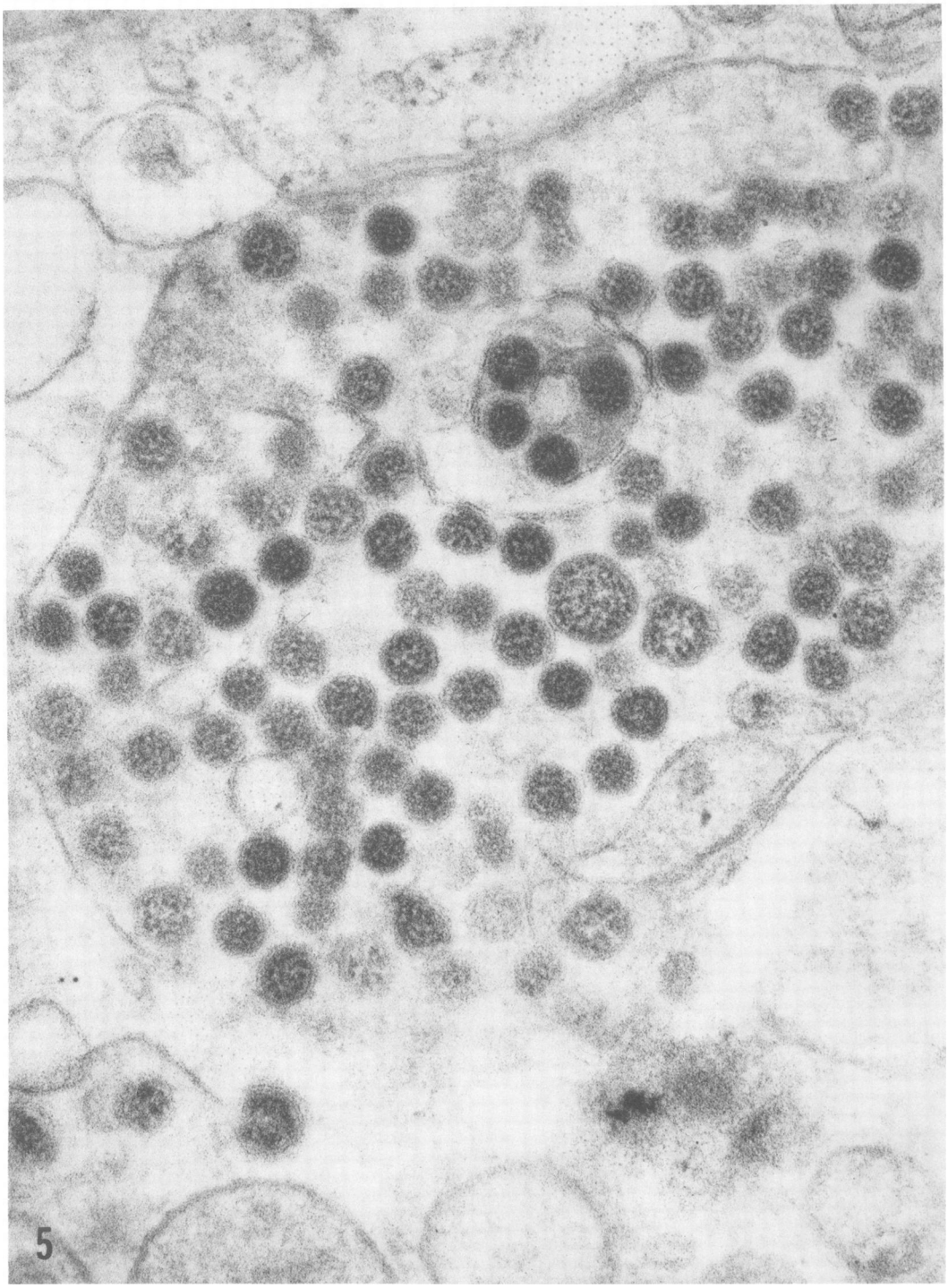

FIG. 5. *Membrane-bound vesicle containing many coronavirus particles. Note the variation in size.* ×*118,700.*

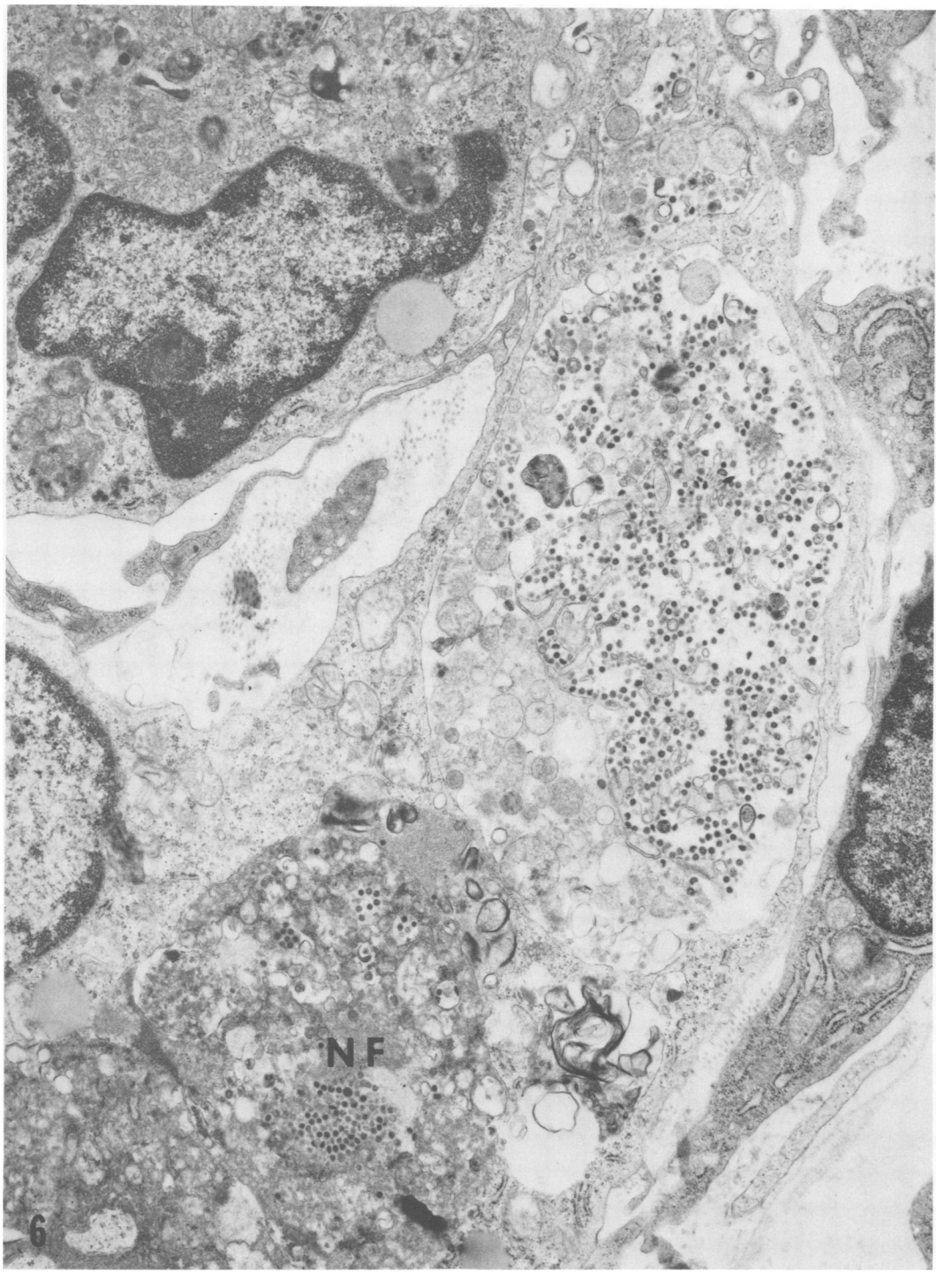

FIG. 6. *Many virus particles are seen within degenerating cells. A cluster of virions is seen within a necrotic focus (NF). ×14,700.*

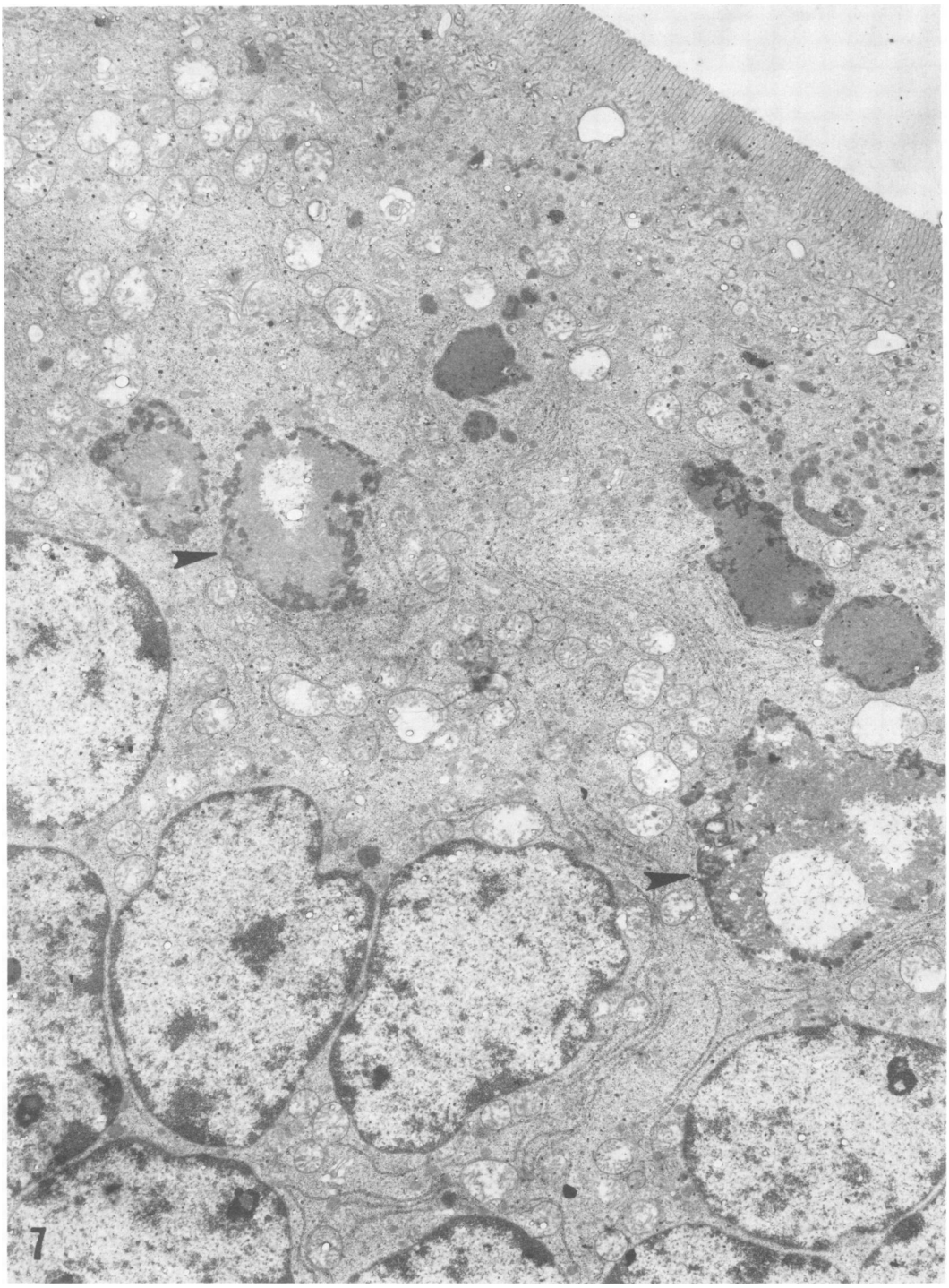

FIG. 7. *Inclusion bodies (arrows) are seen within an intestinal epithelial syncytial cell.* ×*6,500.*

MHV antiserum or with antisera to the other pathogens in CF tests. None of the suspensions exhibited hemagglutination activity.

Virus isolation. Whole intestines from pools of moribund mice were ground to 10 or 20% suspensions with silica in phosphate-buffered

FIG. 8. *Syncytial cell stained with fluorescein-labeled antiserum. The cytoplasm is brightly fluorescent.* ×*800.*

saline and frozen and thawed four times at −70°C to release virus particles from epithelial cells. Uninfected mice harvested at the same age and passage levels provided controls. The homogenates were treated with antibiotics, clarified at 1,000 × *g* for 30 min, and inoculated onto NCTC cells by adsorbing 0.2 ml of the supernatant suspension onto cell monolayers for 1 h at 23°C and then adding 1 ml of MHV maintenance medium to each tube. We observed cell cultures for cytopathology and subpassaged them after one freeze-thaw cycle whenever all cells were affected (4+ cytopathology).

Generally, we isolated the virus in the first passage, although some cultures had to be filtered (0.43 μm) to remove bacterial or yeast contamination. We used virus isolates in fourth and fifth passage levels with infectivity titers of $>10^9$ 50% tissue culture infective doses per ml for all serological and property tests; these tests (described below) were carried out with at least two separate isolations of the virus from this outbreak.

Identification of isolates as Coronaviridae. All viruses isolated had morphology in negative-contrast preparations identical to that of the particles in the crude gut suspensions. Virions were 105 nm (range, 53 to 194 nm) in diameter, including the typical petal-shaped projection layer, and were spherical to highly pleomorphic, with no obvious external or internal symmetry. The viruses did not agglutinate human, rhesus monkey, vervet monkey, cow, sheep, goat, dog, guinea pig, hamster, gerbil, rat, mouse, chicken, turkey, or goose RBC at 4, 23, or 37°C. Infectivity of the isolates was decreased by $\geq 10^6$ by treatment with 0.5% chloroform for 10 min at 23°C, by citric acid at pH 3.0 for 4 h at 23°C, by 0.1% deoxycholate for 30 min at 37°C, and by heating at 50°C for 1 h in MHV maintenance medium. Infectivity was decreased by $10^{3.6}$ after holding in MHV maintenance medium for 24 h both at 23 and at 4°C. Infectivity was totally destroyed by prolonged incubation at 35°C and by a 2-week storage at 4°C. Acridine orange staining of microcultures of the isolates revealed cytoplasmic staining characteristic of single-strand ribonucleic acid viruses. Density of the isolates in sucrose gradients as monitored by electron microscopy was 1.18 to 1.19. Thus, we identified the gut isolates as Coronaviridae by the currently accepted definition of this family (51a).

Identification of isolates as MHV. The isolates reacted the same as crude gut suspensions in CF tests with polyvalent MHV mouse antiserum and did not react with antisera to other murine and human pathogens (Table 1). Furthermore, at their optimal dilution of antigen, the isolates fixed complement to the homologous

TABLE 1. *Relationship of isolates to mouse hepatitis virus and human coronaviruses by CF test*

Antigen	Antiserum[a]							
	MHV-S/CDC				MHV polyvalent (mouse)	HCV[b]		All others[c]
	Pool 3 (mouse)	Pool 4 (mouse)	Pool 5 (mouse)	Pool 6 (mouse)		OC-43 (rabbit)	229E (guinea pig)	
Crude 20% gut suspensions[d]								
LIVIM pool 1 (3rd passage)	128	64	128	64	128	32	<16	<16
LIVIM pool 2 (4th passage)	128	64	128	64	64	16	<16	<16
Normal pool 1 (3rd passage)	<16	<16	<16	<16	32	<16	<16	<16
Virus isolates								
Pool 1 (gut-$NCTC_5$)	64	32	64	32	64	8	<8	<8
Pool 2 (gut-$NCTC_5$)	64	64	64	32	64	8	<8	<8
Normal pool 1 (gut-$NCTC_4$)	<8	<8	<8	<8	8	<8	<8	<8
MHV polyvalent	128	64	128	64	128	32	<8	<8–16
HCV OC-43 (HET_5SMB_{18})	32	16	32	32	32	128	<8	<8
HCV 229E ($\times WI38_1RU_1$)	<8	<8	<8	<8	<8	<8	256	<8
All others[c]	<8	<8	<8	<8	<8–32	<8	<8	64–256

[a] CF antibody titers of the sera are listed in the body of the table as the dilution factor of the highest dilution of serum fixing 5 U of complement overnight with the optimal dilution of antigen as determined in block titrations.

[b] HCV, Human coronavirus strains OC-43 and 229E.

[c] Other murine antigens/antisera tested were: mouse adenovirus, lymphocytic choriomeningitis virus, ectromelia, Sendai virus, reovirus 3, Kilham rat virus, Theiler's GDVII virus, polyoma, K virus, minute virus of mice, Toolan H-1 virus, pneumonia virus of mice, and psittacosis. Human viruses tested included influenza A, B, C; parainfluenza type 1, 2, 3, 4; respiratory syncytial virus; mumps; measles; adenovirus (hexon); herpes simplex; varicella; vaccinia; reovirus 1, 2, 3; coxsackie A (pool) and B (pool); echovirus (pool); rhinovirus (pool); and chlamydia.

[d] 20% suspensions of gut exhibited anticomplementary activity at 1:8 and 1:16 dilutions.

serum titer (1:128) of the MHV polyvalent antiserum, as determined by block titration with MHV polyvalent antigen. Reciprocally, MHV polyvalent antigen at its optimal dilution fixed complement to the homologous serum titer (1:64 or 1:128) of all six pools of MHV-S/CDC antisera, as determined by block titrations with three isolates of the virus. Preepizootic sera from the colony had no detectable CF titers to the isolates. Hence, by the CF test and in reciprocal fashion the isolates were identical to MHV. Furthermore, human coronavirus OC-43, which is known to cross-react with MHV, cross-reacted with MHV-S/CDC antisera to serum CF titers only fourfold lower than the respective homologous titers. In a reciprocal manner, the isolates cross-reacted with OC-43 antiserum to serum titers four- to eightfold lower than the homologous OC-43 titer.

The isolates were similar to MHV in their biological properties as well (18, 35, 46, 49, 51a). The isolates and the five prototype strains of MHV failed to agglutinate a wide variety of RBC at different temperatures. Antisera to the isolates did not have HI activity to a battery of common murine pathogens, but did react by HI to OC-43, as did the MHV polyvalent antiserum (Table 2). The isolates replicated to high infectivity titers (10^7 to 10^{10} 50% tissue culture infective doses per ml) in 2 to 4 days in NCTC-1469 cells, as did the prototype MHV strains. And the isolates, even when degraded by prolonged culturing at 35°C, exhibited one predominant precipitin band in immunodiffusion tests with homologous antisera, the same as found with MHV strains reacting with their homologous antisera.

Relationship of isolates to prototype MHV strains. We performed five separate serological procedures in reciprocal fashion to establish the relationship of the isolates to the prototype MHV strains. The CF test, carried out with complete block titrations of each virus and antiserum, showed reciprocal relationships between the isolates, all MHV strains, and OC-43, the closest relationship occurring between the isolates and strain S (Table 3). The titer between the isolated virus and strain S antiserum was fourfold lower than the homologous strain S titer, but that between S virus and MHV-S/CDC antisera was identical to the homologous MHV-S/CDC serum titer. The titer between JHM virus and MHV-S/CDC antisera

TABLE 2. *Relationship of isolates to hemagglutinating murine viruses and OC-43 by HI test*

System/virus	Antiserum[a]								
	MHV-S/CDC (mouse)				MHV polyvalent (mouse)	HCV OC-43[b]			Homologous[c]
	Pool 1	Pool 2	Pool 3	Pool 6		MIAF[d]	Rabbit	Human	
Chicken RBC, 23°C									
HCV OC-43	32	64	32	32	32	2048	1024	128	—
Ectromelia	0[e]	0	0	0	0	0	0	8	256
Guinea pig RBC, 23°C									
Kilham rat	16	16	16	16	16	8	8	8	1024
Toolan H-1	8	0	0	8	8	0	0	0	512
Sendai	0	0	0	0	0	0	0	8	2048
SV-5	0	0	0	0	0	0	0	0	2048
Human O RBC, 23° C									
Reovirus-3	0	0	0	0	0	0	0	8	1024
Mouse RBC, 23°C									
Minute	0	0	0	0	0	0	0	8	2048
Pneumonia	0	0	0	0	0	0	0	0	2048
Guinea pig RBC, 4 °C									
Polyoma	0	0	0	0	0	0	0	0	1024
Human O RBC, 4°C									
Theiler's GDVII	8	8	8	8	8	0	0	8	1024
Sheep RBC, 4°C									
K	0	0	0	0	0	0	0	0	1024

[a] HI antibody titers of the sera are listed as the dilution factor of the highest dilution of serum inhibiting hemagglutination by 4 hemagglutination units of virus per 0.025 ml for 1 h in the system indicated.

[b] For descriptions of these antisera, see references 23 and 25. HCV, Human coronavirus.

[c] Homologous HI titer of specific rabbit, mouse, horse, chicken, or sheep antiserum for each virus.

[d] MIAF, Mouse immune ascitic fluid.

[e] O = <8.

was twofold lower than the homologous MHV-S/CDC serum titer; all other strains were fourfold lower. Human coronavirus strain 229E was antigenically distinct except for its bilateral cross with MHV-3.

We then employed the serum neutralization test to determine precise interrelationships. We used multiple replicas of each virus-serum combination and calculated serum titers by a logarithmic transformation procedure that interpolated between serum dilutions. We incubated each MHV strain at a virus dilution containing 100 50% tissue culture infective doses per 0.1 ml with each MHV antiserum at dilutions of 1:20 through 1:640 for 1 h at 23°C, and then inoculated 0.2 ml of each mixture in replicas of five onto NCTC-1469 monolayers under fresh MHV-maintenance medium. After 5 days of stationary incubation at 35°C, we read the tests and scored the degree of cytopathology in each monolayer. The scoring system, used with a nomograph constructed from theoretical mean scores versus titer, allowed accurate interpolation between actual serum dilutions. The titers listed are, therefore, more objective (Table 4). The antisera were toxic to the cells at dilutions of 1:10 and occasionally 1:20, so that titers of <1:20 could not be measured.

As shown in Table 4, heterologous serum neutralization titers abound among the MHV strains, but many of the close relationships (heterologous titer within fourfold of the homologous titer) were unilateral. We observed significant but unilateral cross-neutralizations between strains A59 and S and between JHM and 1. The heterologous titer of MHV-S/CDC virus against antiserum to MHV-1 was 9.3-fold lower than the MHV-1 homologous SN titer; that to MHV-3 was 6.1-fold lower than homologous; that to A59 was 6.7-fold lower; that to JHM was 16.5-fold lower; and that to S was 3.1-fold lower. Reciprocally, the heterologous titer of MHV-S/CDC antiserum against MHV-1 virus was 5.2-fold lower than the homologous MHV-S/CDC

TABLE 3. *Relationship of isolates to MHV strains by CF test*

Antigen	Antiserum[a]							
	MHV-1 (mouse)	MHV-3 (mouse)	MHV-A59 (mouse)	MHV-JHM (mouse)	MHV-S (mouse)	MHV-S/CDC (mouse)[b]	OC-43 (MIAF)[c]	229E (guinea pig)
MHV-1 (×$NCTC_2$)	**64**	128	64	8	32	32	8	<4
MHV-3 (×$NCTC_2$)	16	**512**	256	16	32	32	8	8
MHV-A59 (×$NCTC_2$)	8	128	**256**	16	16	32	8	<4
MHV-JHM (×$NCTC_2$)	4	64	32	**64**	16	64	8	<4
MHV-S (×$NCTC_2$)	8	64	16	16	**128**	128	8	<4
LIVIM pool 3 (10% gut)	8	16	32	4	32	**128**	8	<4
Isolate (pool 3) (gut/$NCTC_4$)	4	16	32	4	32	**64**	8	<4
Normal (10% gut)	4	4	8	4	4	4	<4	<4
Normal (gut/$NCTC_4$)	<4	4	4	<4	<4	<4	<4	<4
OC-43 (10% SMB_{14})	4	32	64	8	16	32	**128**	<4
229E (×$RU_{10}HELF_4$)	<4	16	4	<4	<4	<4	<4	**512**

[a] CF antibody titers of the sera are listed in the body of the table as the dilution factor of the highest dilution of serum fixing 5 U of complement overnight with the optimal dilution of antigen as determined in block titrations. Data in boldface are homologous antiserum titers.

[b] Titer listed is the geometric mean titer of antiserum pools 1 and 2.

[c] Mouse immune ascitic fluid (23, 25).

TABLE 4. *Relationship of isolates to MHV strains by serum neutralization test*

Antigen	Antiserum[a]					
	MHV-1	MHV-3	MHV-A59	MHV-JHM	MHV-S	MHV-S/CDC[b]
MHV-1	**195**	70	38	≤20	39	28
MHV-3	≤20	**315**	48	≤20	21	23
MHV-A59	26	74	**514**	≤20	85	27
MHV-JHM	60	36	60	**346**	32	43
MHV-S	≤20	32	22	≤20	**210**	111
MHV-S/CDC[c]	21	52	77	21	68	**147**

[a] Serum neutralization antibody titers are listed in the body of the table as the dilution factor of the highest dilution of serum (as interpolated by a logarithmic transform scoring system) inhibiting infectivity by 30 to 300 50% tissue culture infective doses per 0.1 ml of virus at 5 days. Data in boldface are homologous antiserum titers.

[b] Average by geometric mean titer of data from mouse antiserum pools 1, 2, 4, and 6.

[c] Average by geometric mean titer of data from two isolations of the virus from this epidemic.

SN titer; that against MHV-3 virus was 6.4-fold lower; that against A59 was 5.4-fold lower; that against JHM was 3.4-fold lower; and that against S was 1.3-fold lower. MHV-S/CDC virus, then, is distantly related to MHV strains 1, 3, and A59, unilaterally related to strain JHM, and bilaterally related to strain S.

The SRH test confirmed these results by utilizing type-specific CF rather than neutralization to detect antibody to whole virus. For simplicity, the single radial hemolysis data, which were transformed from diameter of hemolysis zone (in millimeters) to serum CF, serum neutralization, or HI titer via established nomographs (25), are presented here as +++ (homologous zone of hemolysis, equivalent to the homologous serum titer), ++ (equivalent serum titer which is two- to fourfold lower than homologous), + (equivalent serum titer which is >4<16-fold lower than homologous), and − (zone of hemolysis absent or equivalent to a serum titer >16-fold lower than homologous titer). Zones of hemolysis indicating virus-antibody-complement interaction formed for all homologous systems, and again indicated a bilateral relationship between strains S and MHV-S/CDC (Table 5). Other cross-reactions observed by single radial hemolysis including the bilateral cross between OC-43 and all MHV strains, were generally the same as those observed by CF and/or serum neutralization tests.

The immunodiffusion and counterelectropho-

TABLE 5. *Relationship of isolates to MHV strains by single radial hemolysis test*

Antigen[b]	Antiserum[a]							
	MHV-1 (mouse)	MHV-3 (mouse)	MHV-A59 (mouse)	MHV-JHM (mouse)	MHV-S (mouse)	MHV-S/CDC[c] (mouse)	OC-43 (rabbit)	229E (guinea pig)
MHV-1	+++	+	+	−	+	+	+	−
MHV-3	+	+++	+	−	+	+	+	−
MHV-A59	+	+	+++	−	++	+	+	−
MHV-JHM	++	+	+	+++	+	+	+	−
MHV-S	+	+	+	−	+++	++	+	−
MHV-S/CDC[d]	+	+	+	−	+	+++	+	−
Normal control[e]	−	−	−	−	−	−	−	−
OC-43	+	+	+	−	+	+	+++	−
229E	−	+	−	−	−	−	−	+++

[a] Single radial hemolysis titers are listed in the body of the table as +++ (homologous titer), ++ (titer within fourfold of homologous), + (titer >4 < 16-fold of homologous), or − (titer >16-fold of homologous).

[b] All antigens are NCTC-1469 tissue cultures harvested at 2 to 3 days (optimal infectivity) except human coronavirus OC-43 (purified from suckling mouse brain [23]) and human coronavirus 229E (grown in HELF cells [20]).

[c] Average by geometric mean titer of data from antiserum pools 1, 2, 4, and 6.

[d] Average by geometric mean titer of data from two isolations of the virus.

[e] Normal MHV control is fourth passage of a 20% suspension of uninfected pooled suckling mouse gut in NCTC-1469 cells, inoculated and harvested parallel to the epizootic isolates.

resis tests, which by their simplicity are the most direct, albeit the least sensitive, of the procedures used, confirmed the above results. In both tests we expected that a single precipitin line would form near the antigen well in the homologous system, because no "soluble" antigens had been observed in immunodiffusion, counterelectrophoresis, or immunoelectrophoresis tests with MHV cultures. In counterelectrophoresis tests, a precipitin band formed near the virus well for the homologous systems, between MHV-S/CDC virus and antisera to A59, S, and OC-43, and between JHM and S viruses and MHV-S/CDC antisera. In immunodiffusion tests, the precipitin band exhibited a strong partial identity between these reactants and a weak partial identity among all other MHV combinations.

Production of disease with MHV-S/CDC isolates. We inoculated newborn pathogen-free mice orally-intranasally with a loopful of fifth NCTC-1469 cell-culture-passaged virus. The resulting disease was less severe than in the original epizootic. The illness consisted of mild diarrhea without mortality followed by severe runting, which was evident 10 days after exposure. The inoculated mice were thin and smaller than the controls and had ruffled hair coats. Histologically, they showed enteritis but no evidence of liver or brain disease. The mothers of these mice developed CF and single radial hemolysis antibodies to MHV polyvalent antigen and to the isolates. Attempts to produce lethal enteritis with first- and second-passage tissue culture harvests were inconclusive, probably because the virus titers were too low to initiate infection.

Immunity. In all cases, second litters from previously exposed dams were protected from infection after experimental or natural exposure. The runting effects of cell culture inoculums were also ablated. Thus, passive immunity plays an obvious role in checking enteritis in natural settings.

DISCUSSION

We have identified the cause of a 1976 epizootic of lethal enteritis in our colonies as a coronavirus related to the S strain of MHV. The virus was distinct from the S strain but exhibited sufficient antigenic relatedness to be considered a variant or subtype of strain S rather than a totally new type. In this regard, discovery by Rowe et al. (50) of the enterotrophic S strain with distinct intestinal lesions, excretion of virus in feces, and contagiousness by the oral route, is all the more interesting. This earlier S strain, however, caused an enteritis with subsequent hepatitis and encephalitis (35, 46, 49, 50). In our study hepatitis and encephalitis were not seen.

We found no evidence that LIVIM was caused by an interaction of two agents. Electron microscopy revealed only cornavirus particles, and neither CF nor HI tests gave serological evidence of infection by any virus other than MHV. Newborn mice inoculated with tissue culture har-

vests of the isolates developed enteritis and runting, and their mothers developed serological evidence of infection. The singular association of this coronavirus with a specific enteric disease is consistent with Kraft's original description of LIVIM disease; she described many properties of the filtrable agent of LIVIM disease, and all of these properties fit those of our MHV-S/CDC isolates (32). Unfortunately, her agent could not be located for comparative tests.

The MHV-S/CDC strains were serologically related to the other MHV strains and to OC-43. Serological cross-reactions among human and animal coronaviruses are often seen: among various MHV strains (9, 27, 35, 46, 50, 51a) and between MHV and human coronavirus OC-43 (7, 19, 35, 37, 45, 49), between MHV-3 and human coronavirus 229E (7); among MHV, rat coronavirus, and sialodacryoadenitis virus of rats (5, 43); among human coronavirus OC-43, hemagglutinating encephalomyelitis virus of swine, and neonatal calf diarrhea coronavirus of cattle (29, 30, 45); between neonatal calf diarrhea virus and a gastroenteritis coronavirus of horses (3); among transmissible gastroenteritis virus of swine, feline infectious peritonitis virus of cats, and the canine coronavirus 1-71 (31, 45, 48); and among others less well documented (15, 35, 45, 49, 51a).

Since our first report (8), other workers have also found an association between LIVIM disease and MHV infection. A recent note by Carthew describes four out of eight epidemics of diarrheal disease in his colonies in Surrey, England, as due to MHV (these four epidemics are identical to LIVIM disease), one to MHV plus EDIM, one to EDIM alone, and two to reovirus 3 (10). In an epidemic of LIVIM disease in February 1978 in the mouse colony at Yale University, large numbers of coronavirus particles were seen in intestinal contents of moribund sucklings and were identified as MHV (Pravin Bhatt, personal communication, 1978). In a recent epizootic of fatal diarrhea in 10-day-old mice in Japan, LIVIM disease was at first suspected, but necrotic hepatitis was also found; an untyped MHV strain was isolated from gut, liver, and brain specimens (27).

The lesions in the newborn mice infected in the CDC epizootic were identical to those originally described (6, 32, 33), and they are similar to those found in other coronavirus enteridites in animals. Transmissible gastroenteritis of swine is characterized by "villous atrophy"; the virus preferentially infects absorptive epithelial cells near the tips of villi, causing necrosis and severe atrophy or blunting (16, 54). Coronaviruses have been associated with neonatal calf diarrhea; a similar shortening of intestinal villi has been described with consequent decrease in the villus-to-crypt ratio (38, 39). Bluecomb disease coronavirus in turkeys causes shortening of villi and loss of microvilli (14, 47). Enteritis in newborn dogs associated with a canine coronavirus is marked by atrophy and fusion of villi, with a resulting depression of epithelial cell enzyme activities (31).

The severity of MHV infection in sucklings, and lack of clinical disease in adults, are best explained by the ability of older mice to compensate for the rapid loss of intestinal epithelial cells (6). Mice infected during the first 2 weeks of life cannot replace infected and sloughed absorptive epithelium. The result is a severe loss of water and electrolytes, leading to rapid dehydration and death.

The list of diseases associated with coronavirus infection in humans and animals has become especially diverse. Coronaviruses are associated with conjunctivitis (34) and salivary gland infection (5) in rats; upper respiratory illness in humans (17, 28, 35) and rats (5); lower respiratory illness in humans (36), mice (53), rats (5, 43), chickens (35), and pigs (40); kidney disease in humans (1, 15), chickens (35) and pigs (49); liver disease in man (49; A. W. Holmes, F. Deinhardt, W. Harris, F. Ball, and G. Cline, J. Clin. Invest. **49**:45a, 1970) and mice (9, 46, 50); and peritonitis and generalized infection in cats (44, 49) and mice (53). The most severe illnesses involve the central nervous system and the gastrointestinal tract. In mice, central nervous system lesions, including demyelination and neuronal necrosis, have been classically associated with MHV-JHM (2); other MHV strains cause focal to diffuse hepatic necrosis and encephalitis (9, 46, 50), to which athymic (nude) mouse strains are especially susceptible (53). Encephalitis also occurs in cats (49) and pigs (35, 40). Some outbreaks in humans (12) and sheep (52) of nonfatal gastroenteritis in adults may be associated with coronaviruses. Fatal or severe neonatal enteritis is associated with coronavirus infections in horses (3), turkeys (14), pigs (16, 54), dogs (31), cows (38, 39), and, now, mice (8).

The virulence of MHV strains in mouse colonies has long been a subject of practical importance. Host factors and the immune status of animals in closed colonies appear to reduce MHV to a chronic, asymptomatic state. When mice from such colonies come in contact with "pathogen-free" mice, as apparently happened in the epizootic described here, infection becomes fulminant in the highly susceptible newborn mice. The disease produced may depend on the particular strain or strains of virus being carried by the closed-colony adults, or it may be the result of changes in the tropism and patho-

genicity of these viruses. For example, in the enteritis epizootic studied by Rowe et al., the MHV-S strain appeared to lose some of its virulence for CD-1 mice during passage in M and GP mice, and tissue culture isolates (at the eighth passage level) showed markedly decreased pathogenicity (50). We also found a decrease in virulence after tissue culture passage of the MHV-S/CDC isolates (at the fourth and fifth passage levels), but no change in virulence during 16 serial passages per os in suckling mice (i.e., mice exposed at 1 to 2 days of age consistently died in 5 to 7 days with typical enteritis). In our study however, this decreased virulence of tissue culture material may not be significant, for (i) coronaviruses are notoriously labile (20), and (ii) less virus was applied by loop to each mouse than was applied by touching the nose and mouth of a mouse to infectious feces. Electron microscopy data suggest that both events occurred here. Further work is under way to determine whether tropism or pathogenicity changes occur while MHV is latent in adult mice, to assess the role of passive immunity in the latency of MHV, and to accurately measure the attenuation of MHV induced by passage in NCTC-1469 cells.

ACKNOWLEDGMENTS

We thank Erskine Palmer, Gregory Tannock, Patricia Bingham, Mary Flemister, Yvonne Stone, and Sylvia Whitfield for excellent assistance throughout this study.

LITERATURE CITED

1. **Apostolov, K., P. Spasić, and N. Bojanić.** 1975. Evidence of a viral aetiology in endemic (Balkan) nephropathy. Lancet **ii**:1271-1273.
2. **Bailey, O. T., A. M. Pappenheimer, F. S. Cheever, and J. B. Daniels.** 1949. A murine virus (JHM) causing disseminated encephalomyelitis with extensive destruction of myelin. II. Pathology. J. Exp. Med. **90**:195-212.
3. **Bass, E. P., and R. L. Sharpee.** 1975. Coronavirus and gastroenteritis in foals. Lancet **ii**:822.
4. **Bauer, S. P., and F. A. Murphy.** 1975. Relationship of two arthropod-borne rhabdoviruses (Kotonkan and Obodhiang) to the rabies serogroup. Infect. Immun. **12**: 1157-1172.
5. **Bhatt, P. N., R. O. Jacoby, and A. M. Jonas.** 1977. Respiratory infection in mice with sialodacryoadenitis virus, a coronavirus of rats. Infect. Immun. **18**:823-827.
6. **Biggers, D. C., L. M. Kraft, and H. Sprinz.** 1964. Lethal intestinal virus infection of mice (LIVIM). Am. J. Pathol. **45**:413-422.
7. **Bradburne, A. F.** 1970. Antigenic relationships amongst Coronaviruses. Arch. Gesamte Virusforsch. **31**:352-364.
8. **Broderson, J. R., F. A. Murphy, and J. C. Hierholzer.** 1976. Lethal enteritis in infant mice caused by mouse hepatitis virus. Lab. Anim. Sci. **26**:824.
9. **Calisher, C. H., and W. P. Rowe.** 1966. Mouse hepatitis, reo-3, and the Theiler viruses. Natl. Cancer Inst. Monogr. **20**:67-75.
10. **Carthew, P.** 1977. Lethal intestinal virus of infant mice is mouse hepatitis virus. Vet. Rec. **101**:465.
11. **Casey, H. L.** 1965. Standardized diagnostic complement fixation method and adaptation to micro test. Public Health monograph no. 74, Public Health Service, Washington, D.C.
12. **Caul, E. O., and S. I. Egglestone.** 1977. Further studies on human enteric coronaviruses. Arch. Virol. **54**:107-117.
13. **Cheever, F. S., and J. H. Mueller.** 1947. Epidemic diarrheal disease of suckling mice. I. Manifestations, epidemiology, and attempts to transmit the disease. J. Exp. Med. **85**:405-416.
14. **Deshmukh, D. R., J. H. Sautter, B. L. Patel, and B. S. Pomeroy.** 1976. Histopathology of fasting and bluecomb disease in turkey poults and embryos experimentally infected with bluecomb disease coronavirus. Avian Dis. **20**:631-640.
15. **Georgescu, L., P. Diosi, I. Butiu, L. Plavosin, and G. Herzog.** 1978. Porcine coronavirus antibodies in endemic (Balkan) nephropathy. Lancet **i**:163.
16. **Haelterman, E. O.** 1972. On the pathogenesis of transmissible gastroenteritis of swine. J. Am. Vet. Med. Assoc. **160**:534-540.
17. **Hamre, D., and J. J. Procknow.** 1966. A new virus isolated from the human respiratory tract. Proc. Soc. Exp. Biol. Med. **121**:190-193.
18. **Hartley, J. W., and W. P. Rowe.** 1963. Tissue culture cytopathic and plaque assays for mouse hepatitis viruses. Proc. Soc. Exp. Biol. Med. **113**:403-406.
19. **Hartley, J. W., W. P. Rowe, H. H. Bloom, and H. C. Turner.** 1964. Antibodies to mouse hepatitis viruses in human sera. Proc. Soc. Exp. Biol. Med. **115**:414-418.
20. **Hierholzer, J. C.** 1976. Purification and biophysical properties of human coronavirus 229E. Virology **75**:155-165.
21. **Hierholzer, J. C., N. O. Atuk, and J. M. Gwaltney, Jr.** 1975. New human adenovirus isolated from a renal transplant recipient: description and characterization of candidate adenovirus type 34. J. Clin. Microbiol. **1**:366-376.
22. **Hierholzer, J. C., and M. Barme.** 1974. Counterimmunoelectrophoresis with adenovirus type-specific anti-hemagglutinin sera as a rapid diagnostic method. J. Immunol. **112**:987-995.
23. **Hierholzer, J. C., E. L. Palmer, S. G. Whitfield, H. S. Kaye, and W. R. Dowdle.** 1972. Protein composition of coronavirus OC 43. Virology **48**:516-527.
24. **Hierholzer, J. C., M. T. Suggs, and E. C. Hall.** 1969. Standardized viral hemagglutination and hemagglutination-inhibition tests. II. Description and statistical evaluation. Appl. Microbiol. **18**:824-833.
25. **Hierholzer, J. C., and G. A. Tannock.** 1977. Quantitation of antibody to nonhemagglutinating viruses by single radial hemolysis: serological test for human coronaviruses. J. Clin. Microbiol. **5**:613-620.
26. **Holmes, I. H., B. J. Ruck, R. F. Bishop, and G. P. Davidson.** 1975. Infantile enteritis viruses: morphogenesis and morphology. J. Virol. **16**:937-943.
27. **Ishida, T., F. Taguchi, Y. Lee, A. Yamada, T. Tamura, and K. Fugiwara.** 1978. Isolation of mouse hepatitis virus from infant mice with fatal diarrhea. Lab. Anim. Sci. **28**:269-276.
28. **Kapikian, A. Z., H. D. James, Jr., S. J. Kelly, and A. L. Vaughn.** 1973. Detection of coronavirus strain 692 by immune electron microscopy. Infect. Immun. **7**:111-116.
29. **Kaye, H. S., W. B. Yarbrough, and C. J. Reed.** 1975. Calf diarrhea coronavirus. Lancet **ii**:509.
30. **Kaye, H. S., W. B. Yarbrough, C. J. Reed, and A. K. Harrison.** 1977. Antigenic relationship between human coronavirus strain OC-43 and hemagglutinating encephalomyelitis virus strain 67N of swine: antibody responses in human and animal sera. J. Infect. Dis. **135**: 201-209.
31. **Keenan, K. P., H. R. Jervis, R. H. Marchwicki, and L. N. Binn.** 1976. Intestinal infection of neonatal dogs with canine coronavirus 1-71: studies by virologic, his-

tologic, histochemical, and immunofluorescent techniques. Am. J. Vet. Res. **37**:247-256.
32. **Kraft, L. M.** 1962. An apparently new lethal virus disease of infant mice. Science **137**:282-283.
33. **Kraft, L. M.** 1966. Epizootic diarrhea of infant mice and lethal intestinal virus infection of infant mice. Natl. Cancer Inst. Monogr. **20**:55-61.
34. **Lai, Y. L., R. O. Jacoby, P. N. Bhatt, and A. M. Jonas.** 1976. Keratoconjunctivitis associated with sialodacryoadenitis in rats. Invest. Ophthalmol. **15**:538-541.
35. **McIntosh, K.** 1974. Coronaviruses: a comparative review. Curr. Top. Microbiol. Immunol. **63**:85-129.
36. **McIntosh, K., R. K. Chao, H. E. Krause, R. Wasil, H. E. Mocega, and M. A. Mufson.** 1974. Coronavirus infection in acute lower respiratory tract disease of infants. J. Infect. Dis. **130**:502-507.
37. **McIntosh, K., A. Z. Kapikian, K. A. Hardison, J. W. Hartley, and R. M. Chanock.** 1969. Antigenic relationships among the coronaviruses of man and between human and animal coronaviruses. J. Immunol. **102**: 1109-1118.
38. **Mebus, C. A., E. L. Stair, M. B. Rhodes, and M. J. Twiehaus.** 1973. Neonatal calf diarrhea: propagation, attenuation, and characteristics of a coronavirus-like agent. Am. J. Vet. Res. **34**:145-150.
39. **Mebus, C. A., E. L. Stair, M. B. Rhodes, and M. J. Twiehaus.** 1973. Pathology of neonatal calf diarrhea induced by coronavirus-like agent. Vet. Pathol. **10**:45-64.
40. **Mengeling, W. L., and R. C. Cutlip.** 1972. Experimentally induced infection of newborn pigs with HEV strain 67N. Am. J. Vet. Res. **33**:953-956.
41. **Murphy, F. A., and S. G. Whitfield.** 1970. Eastern equine encephalitis virus infection: electron microscopic studies of mouse central nervous system. Exp. Mol. Pathol. **13**:131-146.
42. **Pappenheimer, A. M., and J. F. Enders.** 1947. An epidemic diarrheal disease of suckling mice. II. Inclusions in the intestinal epithelial cells. J. Exp. Med. **85**: 417-422.
43. **Parker, J. C., S. S. Cross, and W. P. Rowe.** 1970. Rat coronavirus (RCV): a prevalent, naturally-occurring pneumotropic virus of rats. Arch. Gesamte Virusforsch. **31**:293-302.
44. **Pedersen, N. C.** 1976. Morphologic and physical characteristics of feline infectious peritonitis virus and its growth in autochthonous peritoneal cell cultures. Am. J. Vet. Res. **37**:567-572.
45. **Pedersen, N. C., J. Ward, and W. L. Mengeling.** 1978. Antigenic relationship of the feline infectious peritonitis virus to coronaviruses of other species. Arch. Virol. **58**: 45-53.
46. **Piazza, M.** 1969. Experimental viral hepatitis. Charles C Thomas, Publisher, Springfield, Ill.
47. **Pomeroy, K. A., B. L. Patel, C. T. Larsen, and B. S. Pomeroy.** 1978. Combined immunofluorescence and transmission electron microscopic studies of sequential intestinal samples from turkey embryos and poults infected with turkey enteritis coronavirus. Am. J. Vet. Res. **39**:1348-1354.
48. **Reynolds, D. J., D. J. Garwes, and C. J. Gaskell.** 1977. Detection of transmissible gastroenteritis virus neutralizing antibody in cats. Arch. Virol. **55**:77-86.
49. **Robb, J. A., and C. W. Bond.** 1979. Coronaviridae. Compr. Virol., vol. 14, in press.
50. **Rowe, W. P., J. W. Hartley, and W. I. Capps.** 1963. Mouse hepatitis virus infection as a highly contagious, prevalent, enteric infection of mice. Proc. Soc. Exp. Biol. Med. **112**:161-165.
51. **Syverton, J. T., and P. K. Olitsky.** 1934. Bacteriological studies on an epizootic of intestinal disease in suckling and newly weaned mice. J. Exp. Med. **60**:385-394.
51a. **Tyrrell, D. A., D. J. Alexander, J. D. Almeida, C. H. Cunningham, B. C. Easterday, D. J. Garwes, J. C. Hierholzer, A. Z. Kapikian, M. R. Macnaughton, and K. McIntosh.** 1978. Coronaviridae: second report. Intervirology **10**:321-328.
52. **Tzipori, S., M. Smith, and T. Makin.** 1978. Enteric coronavirus-like particles in sheep. Aust. Vet. J. **54**: 320-321.
53. **Ward, J. M., M. J. Collins, and J. C. Parker.** 1977. Naturally occurring mouse hepatitis virus infection in the nude mouse. Lab. Anim. Sci. **27**:372-376.
54. **Waxler, G. L.** 1972. Lesions of transmissible gastroenteritis in the pig as determined by scanning electron microscopy. Am. J. Vet. Res. **33**:1323-1328.